Electronic Supplementary Material (ESI) for Chemical Communications.

SUPPORTING INFORMATION

Catalytic Cycle of Carbohydrate Dehydration by Lewis Acids: Structures and Rates from Synergism of Conventional and DNP NMR

Pernille Rose Jensen[a] and Sebastian Meier*[b]

[a]Department of Health Technology, Technical University of Denmark Elektrovej 349, 2800 Kgs. Lyngby, Denmark

[b]Department of Chemistry, Technical University of Denmark, Kemitorvet, Bulding 207, 2800 Kgs Lyngby (Denmark),
E-mail: semei@kemi.dtu.dk

Experimental Details

Materials

Unlabelled fructose, [2-^{13}C]fructose and tin(IV) chloride pentahydrate (98%) and d_6-dimethylsulfoxide were purchased from Sigma-Aldrich (Andover, MA, USA). The radical OX063 was obtained from Oxford Instruments, (Abingdon, UK). The trimeric gadolinium chelate of 1,3,5-tris(N-(DO3Aacetamido)-N-methyl-4-amino-2-methylphenyl)-[1,3,5]triazinane-2,4,6-trione was obtained from GE Healthcare (Amersham, UK).

NMR spectroscopy

Fructose was dissolved in d_6-DMSO at concentrations corresponding to 1 M monomer (80 mg natural abundance and 20 mg [2-^{13}C]fructose in 550 μl final volume) in 1.5 ml Eppendorf safelock tubes. Deuterated water (D_2O) was added to a final volume ratio (v/v) of 15%. Tin(IV) chloride was added to a final carbohydrate:catalyst molar ratio of 5:1. The sample was briefly heated to 70 ºC, cooled on ice and immediately transferred to a Bruker Avance III 600 MHz NMR spectrometer equipped with a BBO smartprobe and thermally equilibrated to -20 ºC, where the sample proved stable on the minutes to hours time scale. Subsequently, the temperature was raised to -5 ºC and to +10 ºC, where ^{1}H NMR spectral appearance was superior to ^{1}H NMR at -20 ºC, but the intermediate **2** decayed on the ~1 hour time scale (see Figure S1, below). The procedure was repeated and the reaction mixture was analysed in a Bruker Avance II 800 MHz NMR spectrometer equipped with a TCI cryoprobe. Alternatively, the reaction mixture could also be produced on ice and incubated at 10 ºC until an aldehyde signal displaying a $^2J_{CH}$ scalar coupling of 30 Hz on the satellites emerged. ^{1}H-^{13}C HMBC and HSQC spectra were acquired with non-uniform sampling (30% acquired increments) of the second dimension. The experiment was repeated using 100 mg natural abundance fructose and acquiring a ^{1}H-^{1}H TOCSY spectrum employing a 10 kHz spinlock for 60 ms and non-uniform sampling (30% acquired increments) of the indirect dimension. Use of non-uniform sampling shortened reaction times to durations, for which the intermediate **2** could be stabilized for analysis with an 800 MHz instrument equipped with a cryoprobe at 10 ºC (see Figure S1).

For kinetic experiments, fructose was dissolved in d_6-DMSO at concentrations corresponding to 1 M monomer (100 mg/550 μl final volume) in 1.5 ml Eppendorf safelock tubes. Deuterated water (D_2O) was added to a final volume ratio (v/v) of 15%. Tin(IV) chloride was added to a final carbohydrate:catalyst molar ratio of 5:1. In situ experiments were performed by immediately transferring reaction mixtures to 5 mm NMR tubes and heating the NMR tubes to the desired temperature in the spectrometer. Reaction progress was followed by recording a series of ^{1}H NMR spectra with 90º flip angle excitation as pseudo-2D spectra in real time. ^{1}H T_1 measurements in the absence of catalyst had indicated relaxation times on the order of 1 second (Figure S6), and an inter-scan relaxation delay of 5 seconds (~5×T_1) between 32 transients per time point was used for reaction tracking. Spectra were recorded on a Bruker Avance III 600 MHz spectrometer equipped with a room temperature smart probe.

Hyperpolarized NMR

Hyperpolarization was achieved through solid state dynamic nuclear polarization (DNP) on 25 mg of [2-^{13}C]fructose in an Oxford instruments HyperSense polarizer at 3.35 T. The self-glassing fructose syrup was flash-frozen in liquid helium in the presence of trityl radical OX063 (27 mM) and trimeric gadolinium chelate of 1,3,5-tris-(N-(DO3A-acetamido)-N-methyl-4-amino-2-methylphenyl)-[1,3,5]triazinane-2,4,6-trione (0.9 mM). Polarization buildup was performed for 3 hours at 1.2 K by microwave irradiation at 93.89 GHz with 100 mW to warrant a maximized signal enhancement. The solid hyperpolarized sample of 1.2 K temperature was washed out of the polarized with 5 mL of water that had been heated until 10 bar pressure had been built up in the dissolution chamber, and 600 μL of the hyperpolarized fructose solution was forcefully injected into 4 mL of a d_6-DMSO solution residing in a 9.4 T NMR spectrometer. The transfer time between polarizer and NMR spectrometer was minimized (below 10 seconds) in order to deliver maximum substrate polarization to the catalytic reaction. The d_6-DMSO solution contained 100 mg tin chloride pentahydrate dissolved in 4 mL of d_6-DMSO. The temperature of the solution was equilibrated to 70 ºC inside a Varian 400 MHz NMR spectrometer equipped with a 10 mm broadband observe probe. Acquisition of a series of one-dimensional ^{13}C NMR spectra using 20° flip angle pulses was initiated prior to substrate injection. One ^{13}C NMR spectrum was acquired every 1 second for 2 minutes. This approach provided a time series of spectra, in which the intermediates **2** and **3** could be reliably integrated.

Data Processing

Thermal NMR spectra were recorded, processed and analysed with Bruker (Fällanden, Switzerland) Topspin software. Hyperpolarized NMR data were acquired with VNMRJ and processed and integrated in the MestReNova software suite (Mestrelab Research, Spain).

Data Analysis

Kinetic data from thermal NMR were fitted as sequential reactions in proFit 7 (Quantum Soft, Switzerland). Errors in the fitted values were determined by experimental replicates. The kinetic model of sequential elementary reactions describes the signal areas of **1**, **3** and **4** as

$$\frac{d[1](t)}{dt} = -k_{1app} \times [1](t),$$

$$\frac{d[3](t)}{dt} = k_{1app} \times [1](t) - k_3 \times [3](t), \text{ and}$$

$$\frac{d[4](t)}{dt} = k_3 \times [3](t),$$

where k_{1app} is the slowest step in the conversion of **1** to **3** and molecules **1**, **3** and **4** are as displayed in Scheme 2. The fits of main text Figure 4A indicate that the simple kinetic model is sufficient to describe the kinetic data. The rates for reversible steps were expected to be poorly defined for the following reasons. Previous observations had shown that the conversion of 1,2 dicarbonyl compounds (such as **3**) to α-hydroxy acids (such as **4**) was irreversible,[1, 2] Spectroscopic data indicated that no NMR-detectable equilibrium between **3** and **4** was formed. Rather, the conversion of **3** to **4** was quantitative (Figure 4A) and any reversible reaction rate would thus be minute. Kinetic data for the previously elusive reaction sequence from **1** to **3** was scrutinized with various kinetic models, indicating that the addition of parameters beyond a sequential model was not required to obtain satisfactory fits (Figure S7). Hyperpolarized NMR data for a two-step conversion of **1** to **3** were thus analysed with a kinetic model of sequential elementary reactions as

$$\frac{d[1](t)}{dt} = -k_1 \cdot [1](t) - R_{[1]} \cdot [1](t) - p \cdot [1](t),$$

$$\frac{d[2](t)}{dt} = k_1 \cdot [1](t) - k_2 \cdot [2](t) - R_{[2]} \cdot [2](t) - p \cdot [2](t),$$

$$\frac{d[3](t)}{dt} = k_2 \cdot [2](t) - R_{[3]} \cdot [3](t) - p \cdot [3](t),$$

where $p = \cos(\alpha)$ and α is the excitation flip angle.

Square brackets indicate the signal areas of the compounds **1**, **2** and **3**. Nonlinear least-squares fitting of the signal areas to these differential equations was conducted in MATLAB using the fmincon function. Opposite to thermal NMR, signals of **1**, **2** and **3** are not regenerated between successive scans in D-DNP but decay through the loss of hyperpolarization due to the approach of equilibrium polarization with time constant T_1, and due to reduction of hyperpolarization to a factor of $p = \cos(\alpha)$ by excitation pulses of angle α. Reaction rate constants, longitudinal relaxation times T_1 for the detected hyperpolarized sites in **1**, **2** and **3** and the angle α for the experiment were determined by fitting. The flip angle was determined in fits to 22°, in good agreement with the nominal setting of 20°. T_1 for the detected hyperpolarized sites in **1**, **2** and **3** were 39(±2) s, 40(±2) s and 40(±1) s, respectively.

The reaction pathway encompassing two sequential dehydrations of **1** to **3** (Scheme S2; Figure S7A) via an enol intermediate **2** can arguably be considered the most plausible pathway: for instance, single and double H/D exchange at the C3 position have been observed for analogous reactions in deuterated protic solvents due to enol formation and reversible keto-enol tautomerism.[3] In order to assess the robustness of the derived rate constants, alternative reaction models were tested. To this end, the differential equations shown above were adapted to reflect the conversions displayed on top of the subpanels in Figure S7A-D. Alternative models included a reversible first step (Figure S7B; with the resulting fitted rate constant for the back-conversion of **2** to **1** that is more than two orders of magnitude smaller than the rate constant for the conversion of **2** to **3**), a parallel formation of **2** and **3** (Figure S7C) and the formation of **3** both from and **1** and **2** (Figure S7D). None of these fits were substantially better than the original fit, as judged from the resultant coefficient of determination (R-squared, see Figure S7). Fits of Figure S7B and Figure S7D invoke additional parameters, which lead to

minor improvements of the R-squared due to adding more parameters than may be justified by the data. These observations are consistent with previous descriptions favouring the unidirectional (irreversible) fitting of D-DNP data from biocatalyic experiments in order to improve the accuracy of the determined rate constants.[4] In these previous studies, only small differences in fitted reaction fluxes were obtained using various models. In the current chemocatalytic study, the three models of Figures S7A, B and D all maintain elemental steps from **1** to **2** and from **2** to **3**. The rate constants for these steps were rather robust for the different models applied, with the first conversion yielding average rate constants of 0.00018($\pm$0.00003) s^{-1} for the three models and the second step yielding average rate constants of 0.15($\pm$0.03) s^{-1}. Fitted flip angles and relaxation rates varied by less than $\pm$ 5% in all four models of Figure S7.

Supplementary Schemes:

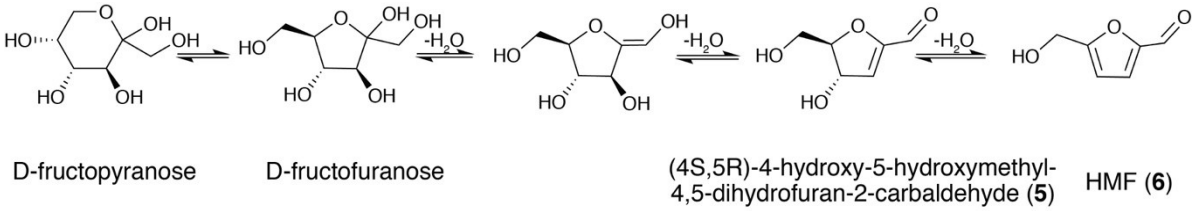

Scheme S1. Schematic depiction of the cyclic pathway via (4S,5R)-4-hydroxy-5-hydroxymethyl-4,5-dihydrofuran-2-carbaldehyde (**5**) to HMF (**6**).

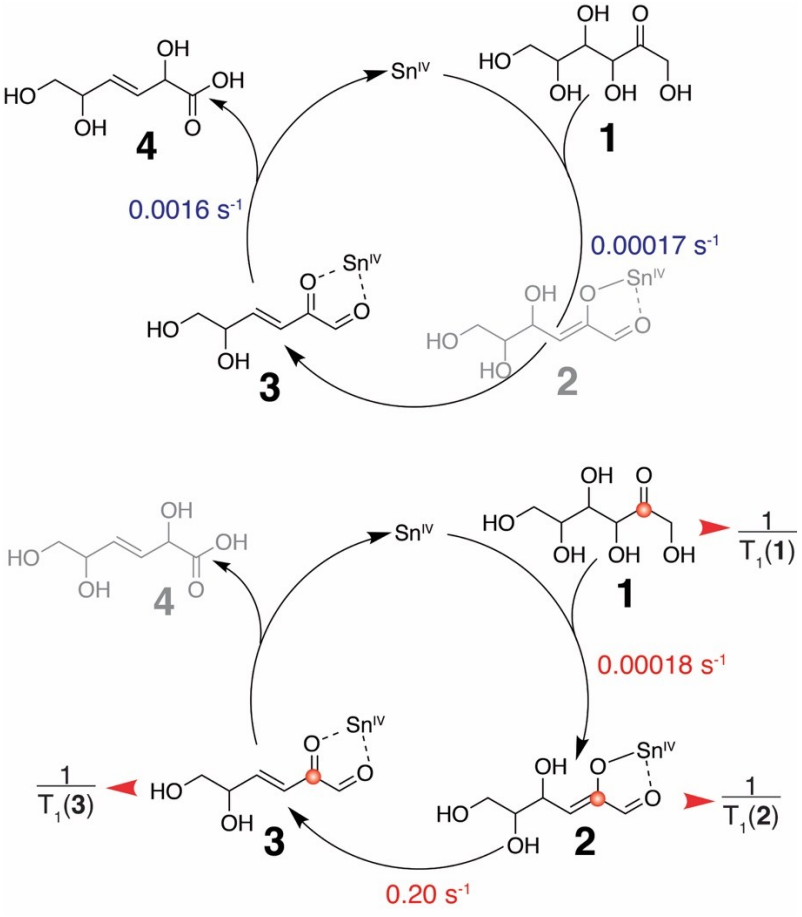

Scheme S2. Schematic overview of rate constants determined through conventional (top) and D-DNP (bottom) NMR.

Supplementary Figures:

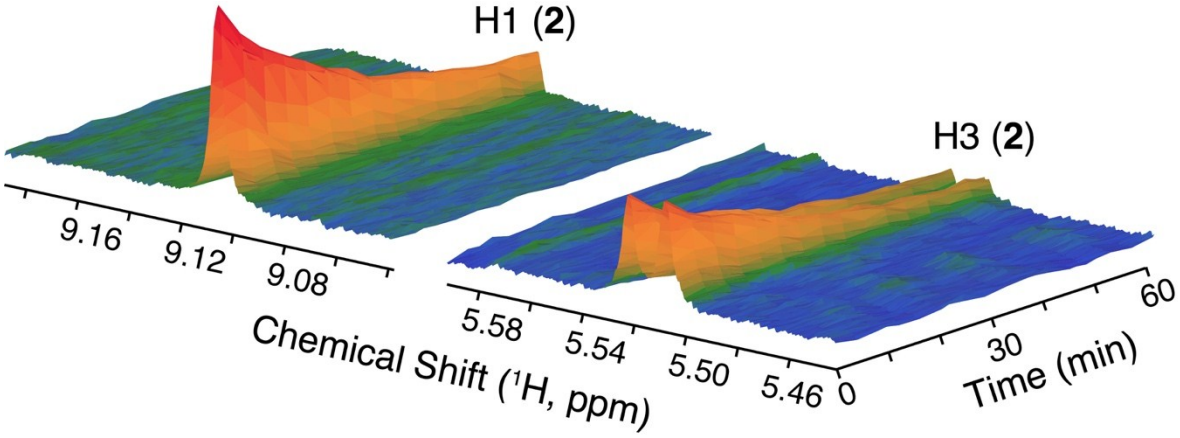

Figure S1. Time series of ^{1}H NMR spectra evaluating the stability of the intermediate **2** at 10 ºC.

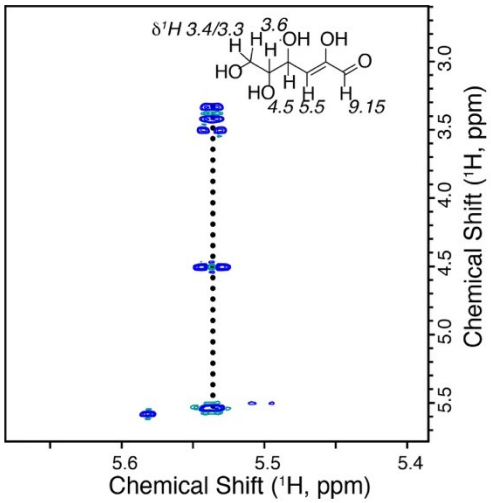

Figure S2. ^{1}H-^{1}H TOCSY NMR spectrum showing the spin system of intermediate **2** (3-DGE, which is the enol tautomer of 3-DG).

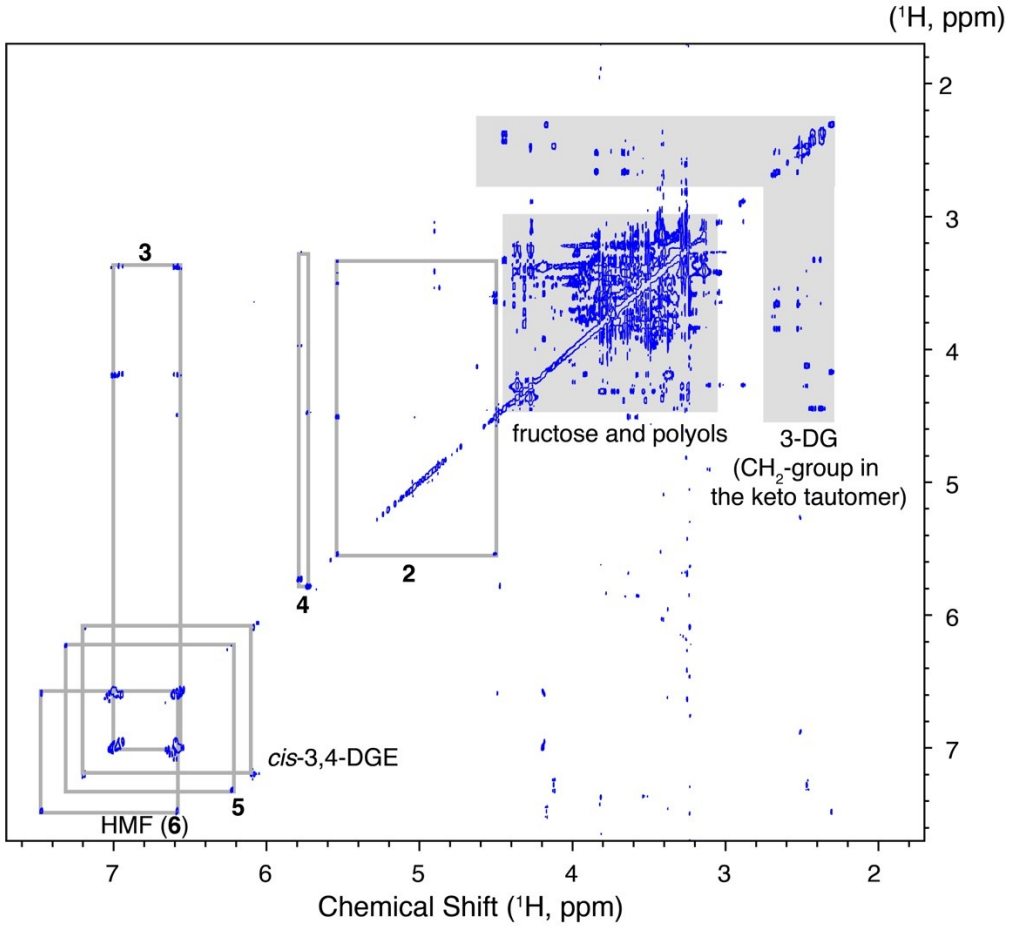

Figure S3. ^{1}H-^{1}H TOCSY NMR spectrum showing spin systems of intermediates formed through acyclic and cyclic pathways (see main text Scheme 2 and Scheme S1) identified on a stabilized sample of the $SnCl_4$-catalyzed conversion of fructose. The identifier **2** designates the enol tautomer 3-DGE (see Fig. S2), while 3-DG designates the corresponding keto tautomer with a CH_2 group at C3, with ^{1}H chemical shifts in the methylene group of 2.2-2.6 ppm. Both fructose and 3-DG exists as various cyclic forms in addition to the acyclic form.

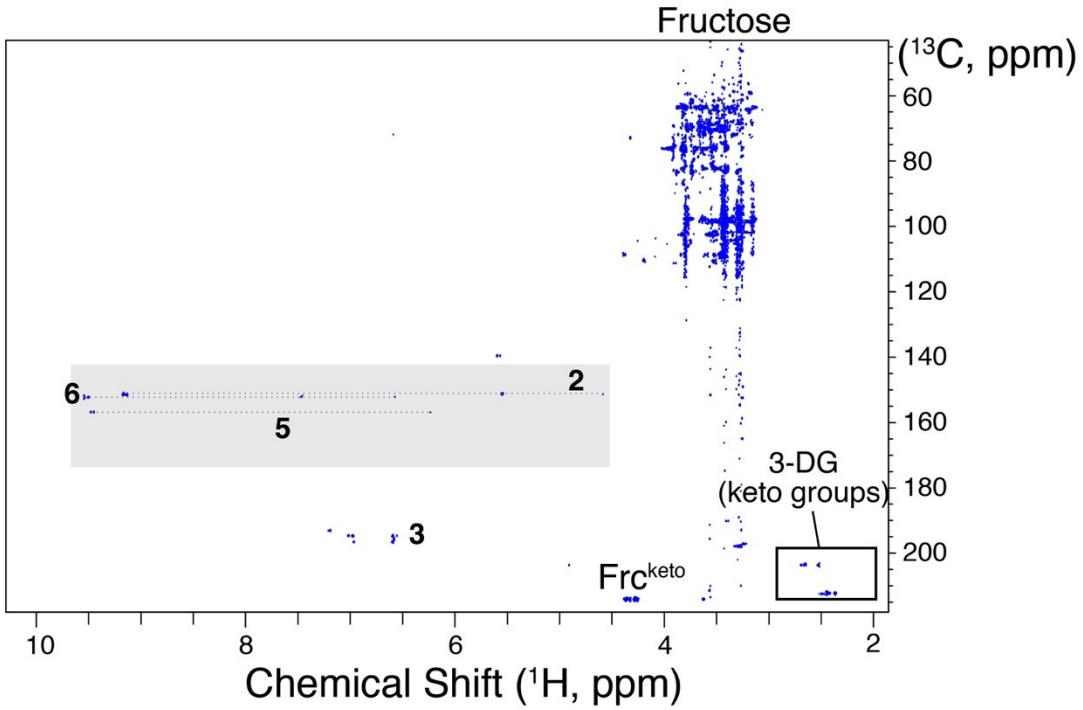

Figure S4. Full ^{1}H-^{13}C HMBC NMR spectrum of a stabilized sample for the $SnCl_4$-catalyzed conversion of 90% fructose/10% [2-^{13}C] fructose. The spectral region of main text Figure 2 is highlighted in grey. 3-DG denotes the keto tautomer of intermediate **2** and two-bond correlations from the CH_2 groups (at C3) to the keto groups at C2 for two major forms of 3-DG are highlighted. Intermediates formed through acyclic and cyclic pathways are labelled by numbers defined in main text Scheme 2 and Scheme S1.

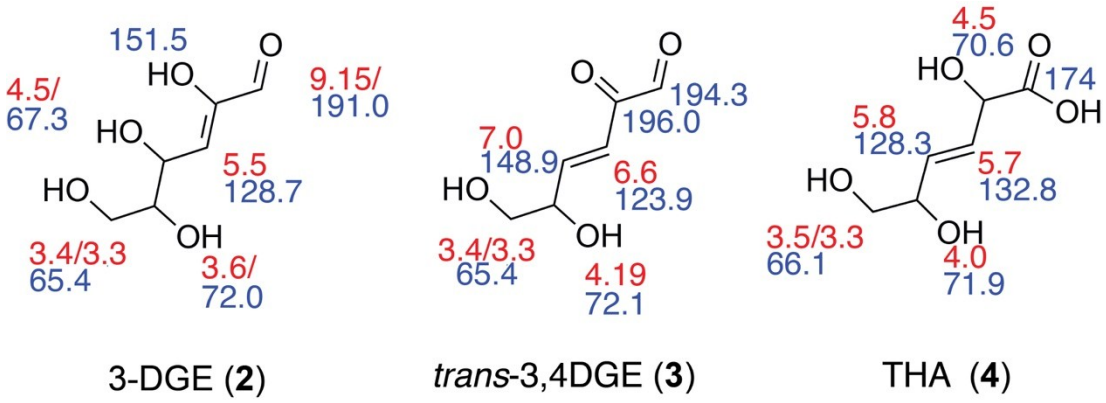

Figure S5. Full chemical shift assignments for compounds **2**-**4**.

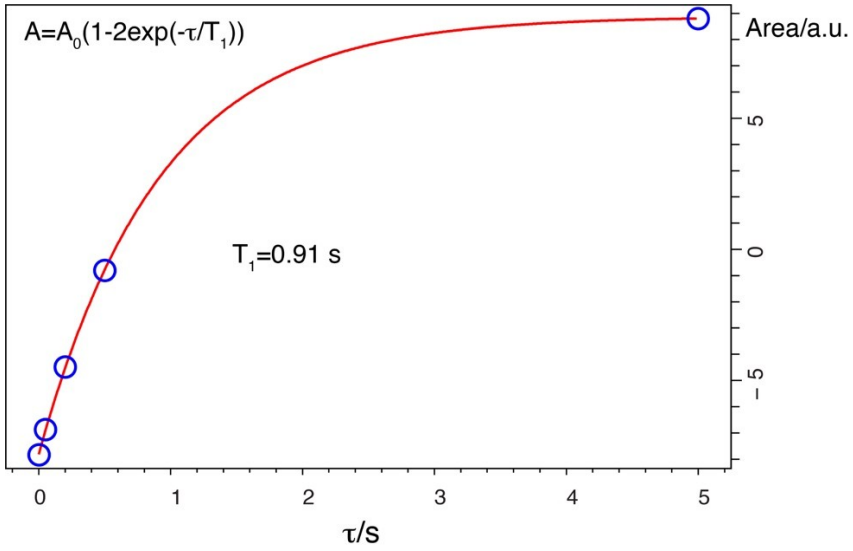

Figure S6. ^{1}H T_1 relaxation measurement for H1 protons in a sample of 1 M fructose in DMSO/D_2O (85%/15%, v/v) at 70 ºC, indicating the suitability of ^{1}H NMR spectra with inter-scan recycle delay of 5 seconds (~5×T_1) to warrant good quantification in reaction tracking experiments of main text Figure 3A.

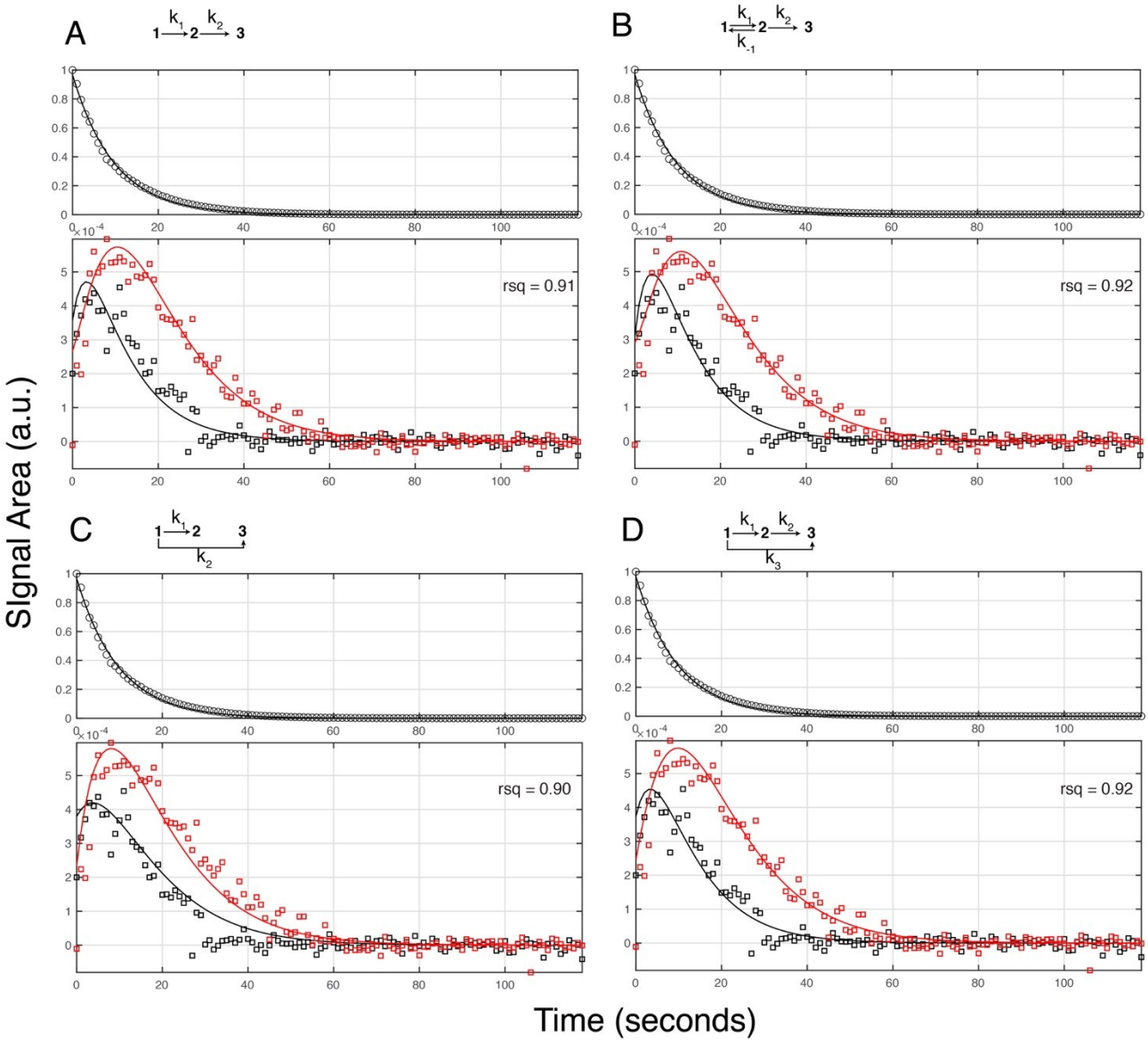

Figure S7. Fit of D-DNP data (black circles: **1**; black squares: **2**; red squares: **3**) to the model described in the main text (A), to a model using a reversible first step (B), a model using a competing formation of **2** and **3** (C), and a model describing the formation of **3** both from **1** and from the intermediate **2**. The coefficient of determination is given as "rsq". Fits indicate that models cannot be proven from the kinetic D-DNP data. Importantly, however, the common rate constants for the conversion of **1** to **2** and of **2** to **3** (in A, B and D) as well as experimental parameters such as flip angle and relaxation times showed only small variations for different models.

References

1. I. Tosi, A. Riisager, E. Taarning, et al., *Catal. Sci. Technol.*, 2018, **8**, 2137-2145.
2. E. A. Pighin, J. I. Di Cosimo and V. K. Díez, *Mol. Catal.*, 2018, **458**, 189-197.
3. P. R. Jensen, E. Taarning and S. Meier, *ChemCatChem*, 2019, **11**, 5077-5084.
4. C. Harrison, C. Yang, A. Jindal, et al., *NMR Biomed.*, 2012, **25**, 1286-1294.